PHYSICAL REVIEW
LETTERS

VOLUME 71 | 18 OCTOBER 1993 | NUMBER 16

Natural Boundaries for Hamiltonian Maps and the Genesis of the Siegel Disk

L. Billi
Scuola Internazionale Superiore di Studi Avanzati, Via Beirut 4, Miramare 34013 Trieste, Italy

G. Turchetti
Dipartimento di Fisica della Università, Via Irnerio 46, Bologna, Italy
and Istituto Nazionale di Fisica Nucleare Sezione di Bologna, Bologna, Italy

Ruifeng Xie
Department of Mathematics, University of Wyoming, P.O. Box 3606, Laramie, Wyoming 82071
(Received 21 April 1993)

The presence of a natural boundary in the angle complex plane of the function conjugating an area preserving map with a rotation is a signature of nonintegrability. Numerical results suggest that the boundary arises from the condensation of singularities when a real nonresonant frequency is approached by a sequence of complex resonant frequencies. For the quadratic map of the complex plane $F:z' = \lambda z + z^2$ the function conjugating the linear part of F with F has q cuts with end points on a spiral if $\lambda = e^{2\pi i p/q - \alpha}$ with $\alpha > 0$. When p/q tends to a (quadratic) irrational number and $\alpha \to 0$ the points coalesce on the boundary of a circle, whose image is the Siegel disk.

PACS numbers: 03.20.+i, 02.30.−f

Recent progress on the theory of Hamiltonian systems [1] has not yet provided a general integrability criterion. The analysis of complex time singularities has been proposed [2] conjecturing that the movable singularities are only poles for integrable systems, branch points with an infinitely sheeted global Riemann surface [3] otherwise. It is still questioned whether on the Riemann surface the singularities are isolated or form a natural boundary [4]. In the algebraic case a rigorous connection with the Arnold-Liouville integrability is proved: The complex time poles are on the lattice defining the complex tori which foliate the complex energy manifold [5,6].

For area preserving maps it was proposed to investigate the singularities of the function which conjugates the complexified system with its normal form. This approach establishes a correspondence between the complex angle and complex time singularities, valid for Hamiltonian flows just as for Hamiltonian maps. For a real analytic map near an elliptic fixed point it was proved [7] that the action singularities are confined to a neighborhood of the real and imaginary axis which they intersect in a set of exponentially small measure; analyticity in a strip is proved for the angle.

Angle analyticity of the conjugation function for an invariant curve was investigated on models like the standard map and semistandard map with real frequencies below the critical breakup value. The standard map is a well known Hamiltonian model corresponding to a kicked pendulum, defined by $r' = r + \epsilon \sin\theta$, $\theta' = \theta + r'$ and can be locally conjugated to a rotation when the frequency (rotation number) Ω satisfies a diophantine condition $|q\Omega/(2\pi) - p|^{-1} \le \gamma |q|$ for all the integer p and q, or has a nonvanishing imaginary part. A local change of coordinates $r = \Omega + \epsilon v(\Omega,\Theta;\epsilon)$, $\theta = \Theta + \epsilon u(\Omega,\Theta;\epsilon)$, where u,v are analytic in a strip of the complex Θ plane, allows giving the map the integrable form $\Omega' = \Omega$, $\Theta' = \Theta + \Omega$. The global analyticity structure of the conjugation functions u,v is relevant because it is related to the time analyticity of the interpolating flow: Indeed the iteration of the map in the new coordinates $\Theta_n = \Theta_0 + n\Omega$ allows being interpolated by $\Theta(t) = \Theta_0 + t\Omega$ where t is real or even complex. As a consequence in the initial coordinates such interpolation reads $\theta(t) = \Theta_0 + t\Omega + \epsilon u(\Omega,\Theta_0 + t\Omega;\epsilon)$, $r(t) = \Omega + \epsilon v(\Omega,\Theta_0 + t\Omega;\epsilon)$, where Ω and Θ_0 depend on the

0031-9007/93/71(16)/2513(4)$06.00

initial conditions r_0, θ_0, and therefore the singularities in t are simply related to the singularities in Θ of u,v.

The semistandard map is a simplified version of the standard map, which consists in replacing the $\sin\theta$ nonlinearity with $e^{i\theta}$, namely $r'=r+\epsilon/(2i)e^{i\theta}$, $\theta'=\theta+r'$. These maps are close to each other when $\mathrm{Im}\theta\ll 0$, as can be checked by inspecting their orbits. The numerical exploration of the singularities in Θ of the conjugation function u for the standard or semistandard map is possible using Padé approximants on the series in $z=e^{i\Theta}$ and z^{-1}. Extended accuracy arithmetic has to be used in order to avoid noise poles due to round off [8,9]. For the semistandard map with real nonresonant frequency the conjugation function appeared to be analytic in a strip whose image has fractal boundaries [10,11]. For the standard map we found that for a complex frequency with resonant real part $\omega/2\pi=p/q$ the singularities provided by the Padé approximants are two families of q half lines parallel to the imaginary axis in any vertical strip of width 2π; such singularity lines allow an analyticity horizontal strip. When the imaginary part tends to zero and real part of the frequency approaches a diophantine value the vertical lines become dense, and their end points are a natural boundary for the analyticity strip since no analytic continuation beyond this boundary is possible.

In this Letter we examine a simplified model, such as the quadratic map, whose features are similar to the semistandard map. As a consequence if we choose ϵ small and $\mathrm{Im}\theta$ large positive or negative the singularity structure found for the standard map is almost the same as for the quadratic map.

For the complex quadratic map we describe analytically the singularity structure of the conjugation function and the rise of the natural boundary. We recall that

$$z'=F(z)\equiv\lambda z+z^2, \tag{1}$$

with $\lambda=e^{i\omega}$ and $\omega/2\pi$ diophantine, is conjugated with its linear part $\zeta'=\lambda\zeta$ in a disk of the ζ plane, whose image in the z plane is called the Siegel disk. This is a connected component of the Julia set $\mathcal{J}$, given by the trajectory of the critical point of $F(z)$, where $F'(z)=0$ and F is locally noninvertible [12]. The Julia set is the basin boundary of ∞; in the cases we consider, $|\lambda|<1$, the Julia set $\mathcal{J}$ is connected and the stability domain having $\mathcal{J}$ as boundary is called the Fatou set $\mathcal{F}$. Letting $z=\Phi(\zeta)=\zeta+O(\zeta^2)$ be the conjugation function and $\zeta=\Psi(z)=z+O(z^2)$ its inverse, the functional equations they satisfy read

$$F\circ\Phi(\zeta)=\Phi(\lambda z),\quad \Psi\circ F(z)=\lambda\Psi(z), \tag{2}$$

and hold for a complex frequency $\omega+i\alpha$ as well.

The circle map $\theta'=\theta+\omega+\epsilon\sin\theta$ when $\mathrm{Im}\theta\ll 0$ is well approximated by the map

$$z'=e^{i\omega}z\exp(ze^{-i\omega}) \tag{3}$$

by setting $z=\epsilon e^{i(\theta+\omega)}/2$. The map (1) has the same qualitative behavior as (3); close to the origin ($|\epsilon|$ small enough) their orbits are indistinguishable and their critical points differ by a factor 2. When $\mathrm{Im}\theta\gg 0$ then the circle map is well described by (3) with $\omega\to-\omega$ by setting $z=\epsilon e^{-i(\theta+\omega)}/2$.

Choosing in Eq. (1) $\lambda=e^{i\omega-\alpha}$ with $\alpha>0$ a lower bound to the convergence radius r_s of Φ is $\frac{1}{4}|\lambda|(1-|\lambda|)$, while a better estimate for $\alpha\to 0$, when $\omega/2\pi$ is diophantine (quadratic irrational) $|e^{ik\omega}-1|^{-1}\le\gamma|k|$, is given by $\gamma^{-1}+\alpha$; for a good numerical algorithm see [13]. When $\omega/2\pi$ is rational then $\gamma^{-1}=0$ and r_s vanishes as $\alpha\to 0$ since the map is no longer linearizable.

When $\omega=0$ and λ is real Φ is analytic in the cut ζ plane as first suggested by a numerical investigation based on Padé approximants [8]. If $0<\lambda<1$ the function Ψ is given by

$$\Psi(z)=\lim_{n\to\infty}\frac{F^{\circ n}}{\lambda^n} \tag{4}$$

and the Julia set $\mathcal{J}$ is a natural boundary of $\Psi(z)$. With $F^{\circ n}$ or $F^{\circ -n}$ we denote the composition of the function F or its inverse F^{-1} with itself n times. In order to determine the analytic structure of $\Phi(\zeta)$ we observe that Ψ does not have a unique inverse in the interior of $\mathcal{F}$.

The critical point of F and all its preimages are critical points of Ψ. Let us denote with $z_c=-\lambda/2$ the critical point and with

$$\begin{aligned} &z_0=z_c,\quad z_k=F_k^{-1}(z_c),\ldots,\\ &z_{k_1,\ldots,k_n}=F_{k_n}^{-1}\circ\cdots\circ F_{k_1}^{-1}(z_c),\quad k_i=1,2, \end{aligned} \tag{5}$$

its preimages

$$F_{1,2}^{-1}(z)=\frac{-\lambda\pm\sqrt{\lambda^2+4z}}{2}. \tag{6}$$

We observe that differentiating the second equation (2) we have

$$\Psi'(F(z))F'(z)=\lambda\Psi'(z), \tag{7}$$

which implies $\Psi'(z_c)=0$, since $\Psi(z)$ is analytic (Ψ' bounded) at $z=F(z_c)$. Differentiating the equation $\Psi(F^{\circ n}(z))=\lambda^n\Psi(z)$ and evaluating it for $z=F^{\circ -n}(w)$ we have

$$\Psi'(w)\prod_{k=1}^{n}F'(F^{\circ -k}(w))=\lambda^n\Psi'(F^{\circ -n}(w)) \tag{8}$$

and therefore $\Psi'(z)$ vanishes at the preimages $z_{k_1,\ldots,k_n}$ of the critical point.

The analytic structure of Φ then emerges if we notice that any of the 2^n preimages $z_{k_1,\ldots,k_n}$ is mapped into the same point ζ_n according to

$$\begin{aligned} &\zeta_c=\Psi(z_c),\quad \zeta_1=\Psi(z_{k_1})=\lambda^{-1}\zeta_c,\ldots,\\ &\zeta_n=\Psi(z_{k_1,\ldots,k_n})=\lambda^{-n}\zeta_c. \end{aligned} \tag{9}$$

In fact replacing in (2) $z=F^{-1}(w)$ we have

$$\Psi(F^{-1}(w)) = \lambda^{-1}\Psi(w)$$

and consequently

$$\Psi(F^{\circ -n}(w)) = \lambda^{-n}\Psi(w).$$

At any of the points ζ_n there is a square root type of singularity. As a consequence Ψ is a one to one analytic map of the Fatou set $\mathcal{F}$ not with the ζ plane but with an infinitely many sheeted Riemann surface obtained as follows: At the square root branch point ζ_c we glue two sheets; the point ζ_1 is a square root branch point in both the previous sheets and in any of them two new sheets are glued and so on *ad infinitum*.

The function Φ has a cut joining ζ_c with ∞ with new branch points at $\lambda^{-1}\zeta_c, \ldots, \lambda^{-n}\zeta_c, \ldots$. Any one of these sheets of the global Riemann surface is mapped by Φ into a domain delimited by arcs, which are the images by Φ of the segments $[\zeta_{n-1}, \zeta_n]$ in all the corresponding Riemann sheets. For instance $[\zeta_c, \zeta_1]$ belongs to two Riemann sheets and is mapped into the segments $[z_c, z_1], [z_c, z_2]$, while $[\zeta_1, \zeta_2]$ which belongs to four Riemann sheets is mapped into the arcs with ends (z_1, z_{11}), (z_2, z_{21}), (z_2, z_{12}), (z_1, z_{22}) and so on. These arcs limit closed domains, each of which has a limit point belonging to $\mathcal{J}$. For instance the cut ζ plane is mapped into a domain of the z plane limited by the curves (union of a numerable sequence of arcs) $\Gamma = [z_c, z_1] \cup (z_1, z_{11}) \cup (z_{11}, z_{111}), \ldots$ and $\Gamma' = [z_c, z_2] \cup (z_2, z_{21}) \cup (z_{21}, z_{211}), \ldots$.

In Fig. 1(a) we exhibit the Julia set with all the above described arcs and the domains where Ψ is single valued. Any of them is mapped into a sheet of the global Riemann surface of Φ. The figure reminds the tasselation of the Poincaré disk with respect to a Fuchsian group. This is not surprising since the dynamics is hyperbolic and we achieve a uniformization process by introducing these domains, which tasselate the Fatou set and are mapped into each other by the action of F_1^{-1} and F_2^{-1}. If $\lambda = e^{i(\omega + i\alpha)}$ is complex the branch points of $\Phi(\zeta)$ are on a spiral and we cut the ζ plane along half lines drawn by projecting them from the origin. The possibility of

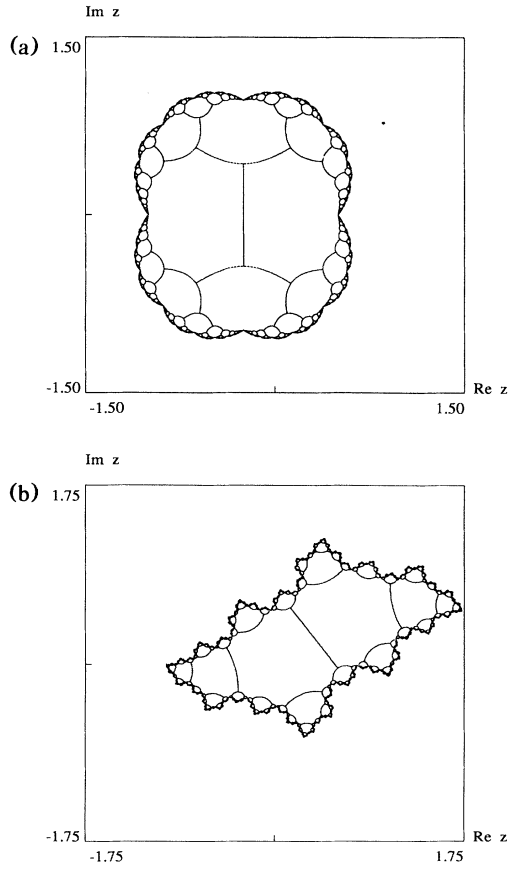

FIG. 1. Domains where the function $\Psi(z)$ is single valued for the map $z' = \frac{1}{2}z + z^2$ (a) and for the map $z' = \frac{9}{10}e^{2\pi i 3/5}z + z^2$ (b).

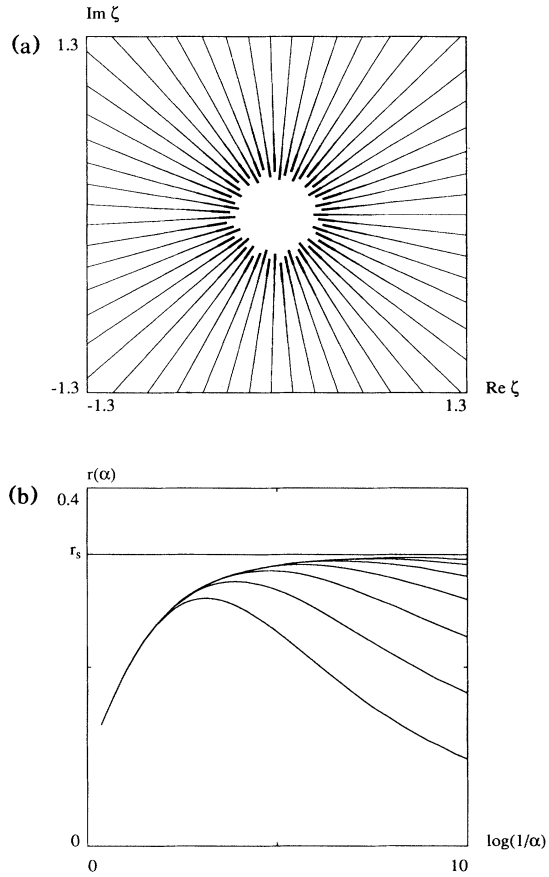

FIG. 2. Pictorial representation of the cuts for the map $z' = 0.994e^{2\pi i 34/55}z + z^2$ (a). Plot of the convergence radius $r_j(\alpha)$ versus $\ln(1/\alpha)$ for the quadratic map with frequencies $2\pi q_{j-1}/q_j + i\alpha$ for $4 \le j \le 10$, where $q_1 = 1, q_2 = 2$, $q_{j+1} = q_{j-1} + q_j$ define the approximations to the golden mean. The horizontal line corresponds to the exact value of the Siegel radius r_S (b).

TABLE I. Values corresponding to the maxima $\alpha=\alpha_j$ of Fig. 2(b).

q_j	$e^{-\alpha_j}$	$\ln(1/\alpha_j)$	$r_j(\alpha_j)$
5	0.96	3.2	0.277
8	0.98	3.9	0.2961
13	0.9915	4.76	0.3081
21	0.9965	5.65	0.3184
34	0.9985	6.50	0.3190
55	0.9995	7.60	0.3214
89	0.9998	8.51	0.3229
		r_{exact}	0.326

joining all the branch points with a spiral will not be considered here. The structure of the Riemann surface and the shape of the domains where Ψ is injective are simple if $\omega/2\pi=p/q$ is a rational number, where we assume p and q prime to each other. The number of cuts in this case is finite and any of them there has a sequence of branch points $\zeta_k,\zeta_{k+q},\ldots,\zeta_{k+mq},\ldots$, for $k=0,\ldots,q-1$. The Riemann surface of Φ is built by suitably gluing the sheets and the corresponding tasselation of the Fatou set $\mathcal{F}$ into domains where Ψ is single valued is shown by Fig. 1(b) for $p=3$, $q=5$. Each domain has q distinct points on $\mathcal{J}$ since the first sheet (and all the others) is divided into q sectors where ∞ can be separately reached. The presence of q cuts and their location is fully confirmed by the distribution of poles of Padé approximants [8,14].

In the case of a nonresonant frequency the number of cuts is infinite and infinite is the number of points belonging to $\mathcal{J}$ in any of the domains tasselating $\mathcal{F}$. Numerical results show an ordered structure with rays of singularities corresponding to the rational approximations p_j/q_j of the continued fraction expansion of $\omega/2\pi$. If we approximate $\omega+i\alpha$ with the sequence $2\pi p_j/q_j+i\alpha$, keeping α fixed, the limit as $j\to\infty$ is better understood. The case of a real diophantine frequency is subsequently obtained by taking the limit $\alpha\to 0$: The branch points coalesce on a circle, creating a natural boundary in all the sheets, which become totally disconnected. A unique limit is obtained by considering the sequence $2\pi p_j/q_j+i\alpha_j$ where α_j converges to 0 for $j\to\infty$.

The best choice α_j is suggested by Table I and Fig. 2(b) where we have plotted the convergence radius $r_j(\alpha)=|\zeta_c|$ of Φ for the golden mean. Since $r_j(\alpha)$ vanishes both for $\alpha\to 0$ and $\alpha\to\infty$ for any j, it has a maximum at some point $\alpha=\alpha_j$. The sequence α_j monotonically decreases to zero and $r_j(\alpha_j)$ monotonically converges to the Siegel radius. The genesis of the Siegel disk, pictorially described by Fig. 2(a), is clear: Φ at step j is analytic in the ζ plane cut along q_j rays collapsing to a circle when $j\to\infty$; $\mathcal{F}$ is no longer simply connected and the domains tasselating $\mathcal{F}$ become its simply connected components. The first component containing the origin becomes the Siegel disk, mapped into the disk $|\zeta|\le r_s$ of the first ζ plane; its boundary is the closure of the orbit of the critical point in agreement with Herman's theorem [12]. The disks in the remaining Riemann sheets are mapped into the simply connected components of $\mathcal{F}$.

This construction shows how the natural boundary of Φ for the real frequency map emerges from the singularity pattern of Φ for the approximating sequence of maps with complex frequencies.

The numerical results for the standard map show that the singularity pattern in the complex angle plane is the same and confirm the crucial role of resonances once the "real" dynamics is approached from "complex dynamics."

We would like to thank Dr. A. Bazzani for very constructive criticism and many useful discussions. One of us (R.X.) would like to thank World Lab for a fellowship which allowed this work to be started.

[1] *Dynamical Systems*, edited by D. V. Anosov and V. I. Arnold, Encyclopedia of Mathematical Sciences (Springer-Verlag, Berlin, 1988).
[2] U. Frish and R. Morf, Phys. Rev. A **23**, 2637 (1981).
[3] Y. F. Chang, M. Tabor, and J. Weiss, J. Math. Phys. **23**, 531 (1982).
[4] D. Bessis and N. Chafee, in *Chaotic Dynamics and Fractals*, edited by M. F. Barnsley and S. G. Demko (Academic, New York, 1986).
[5] M. Adler and P. Van Morbeke, Adv. Math. **38**, 267 (1980).
[6] M. Adler and P. Van Morbeke, Adv. Math. **38**, 318 (1980).
[7] A. Bazzani and G. Turchetti, J. Phys. A **25**, L427 (1992).
[8] R. Xie, in *Chaos: Theory and Practice*, edited by T. Bountis (Springer-Verlag, Berlin, 1993).
[9] J. Gilewicz and B. Truong-Van, in *Constructive Theory of Functions,* Proceedings of the International Conference of Varma, May 1987 (Bulgarian Academy of Sciences, Sofia, 1988).
[10] I. C. Percival and J. M. Greene, Physica (Amsterdam) **3D**, 530 (1981).
[11] I. C. Percival, Physica (Amsterdam) **6D**, 67 (1982).
[12] M. Herman, Commun. Math. Phys. **99**, 593 (1985).
[13] S. Marmi, J. Phys. A **23**, 3447 (1990).
[14] L. Billi, Physics Department thesis, Bologna University, 1992.